Large-eddy simulation of thermal striping in unsteady non-isothermal triple jet

S. Chacko[†], Y. M. Chung[†,*], S. K. Choi[‡], H. Y. Nam[‡], and H. Y. Jeong[‡]

† School of Engineering and Centre for Scientific Computing, University of Warwick,

Coventry CV4 7AL, U.K.

‡ Fast Reactor Technology Development Division, Korea Atomic Energy Research Institute,

Daejeon, Korea

[Final Manuscript]

Abstract

Unsteady temperature fluctuations of non-isothermal turbulent jets are encountered in many engineering applications including liquid metal cooled fast reactors (LMFR), and can cause thermal stresses on solid boundaries. An accurate prediction of the temperature fluctuations is important to assess potential thermal fatigue damage to components, and traditionally this has been done by RANS turbulence modelling calculations with limited success. In this study, a large eddy simulation (LES) technique was applied to

*Corresponding author: Y.M.Chung@warwick.ac.uk

predict the temperature fluctuations of thermal striping observed in a triple jet. The triple jet model was used as a mock-up of the outlet of fuel subassemblies in a nuclear fast reactor. The results show that LES predicted the highly oscillatory nature of unsteady thermal mixing of the triple jet. The LES results were in good agreement with the available experimental data in terms of mean, RMS, skewness and kurtosis. The large amplitude of the temperature fluctuations associated with the thermal striping was captured correctly, demonstrating that LES can be used to analyse unsteady characteristics of thermal striping. Instantaneous and time mean thermal fields were further analysed to assess the capability and accuracy of LES in the thermal striping study. The Spalart-Allmaras and realizable $k-\varepsilon$ turbulence models were also considered along with LES. It is found that these turbulence models produced a very small amplitude of fluctuations, and failed to predict the correct magnitude of unsteady thermal fluctuations, highlighting the limitations of the RANS approach in unsteady heat transfer simulations.

Keyword: triple jet, thermal striping, mixing, thermal fatigue, LES

1 Introduction

Non-isothermal turbulent jets generate an intense mixing of different temperature fluids before they develop fully further downstream, resulting in strong temperature variations in time. Thermal striping refers to these temperature fluctuations that are observed at the interface between the two non-isothermal jets. This phenomenon has been encountered in many engineering applications including liquid metal cooled fast reactors (LMFR), where severe temperature fluctuations occur from the mixing of high and low temperature sodium flowing across the reactor core subassemblies. The temperature difference between the flow streams emanating from the fuel subassemblies and the control rod subassemblies depends on the reactor core design, and it can be as large as 100 °C [1]. The large temperature fluctuations are a primary cause for thermal stresses in the LMFR, and can result in thermal fatigue failure. Therefore, the thermal striping is one of the major factors to consider in the design and life management of components of LMFR, and understanding this phenomenon is important in maintaining high safety standards in LMFR. An accurate heat transfer analysis is required to find its effects on the solid boundary where the fluid temperature changes rapidly and cyclically.

Thermal striping has been studied experimentally with air, water and liquid sodium as a working fluid. Wakamatsu et al. [2] carried out an experiment to understand the thermal striping observed in a fast reactor. Their experiment was designed to reproduce a similar condition in the upper plenum of an LMFR. Hot and cold water was injected through two rectangular nozzles, and a solid plate was placed at a small distance above the nozzles. As the two parallel jets at different temperatures impinged on the solid plate,

the incomplete mixing of hot and cold jets of fluid gave rise to temperature fluctuations as large as about 60% of the discharge temperature difference. It was found that the peak-to-peak amplitude of the surface temperature fluctuations was about half of that of the fluid around the solid plate. Tenchine and co-workers [3–6] performed a series of co-axial jet experiments with air, water and sodium. They found that the air tests can be used to predict the thermal fluctuation behaviour in the sodium reactor [5]. A parallel triple jet configuration has also been used for thermal striping studies [7–10]. Kimura and co-workers [7–9] used a cold fluid in the centre and hot fluid on both sides to model the configuration of the reactor core outlet of control rods surrounded with fuel subassemblies. They used both water and sodium as a working fluid. Recently, Nam and Kim [10] used an air triple jet as a mock-up of the outlet of LMFR fuel subassemblies. Large temperature fluctuations were measured in their experiment with various combinations of inlet velocity and temperature. These experimental studies have provided valuable information in understanding the underlying physical mechanism responsible for thermal striping, but it has been largely limited to relatively simple geometries.

There has been a continual effort to predict the temperature fluctuations in thermal striping using numerical simulations with a view to developing numerical methods applicable to more realistic geometries. Many variants of turbulence models have been used in Reynolds-Averaged Navier-Stokes (RANS) simulations with some varying successes in terms of predicting mean velocity and thermal fields [8, 11–16]. Recently, Choi and Kim [15] performed numerical simulations of the triple jet experiments conducted by Nam and Kim [10]. They found that only the $\overline{v^2} - f$ model [17] was able to predict the temperature fluctuations, while other turbulence models resulted in a steady state

flow. Improved RANS results were reported with grid refinement [14]; the SST $k-\omega$ model [18] also predicted temperature oscillation, albeit small, and an increased level of temperature fluctuations were produced by the $\overline{v^2}-f$ model. However, the predicted amplitude of the temperature fluctuations was still smaller than the experimental value. Despite recent successes with RANS, none of the turbulence models tested were able to predict the correct level of temperature fluctuations, indicating the limited capability of the RANS approach to predict the main cause of thermal striping fatigue damage in LMFR structures.

In this study, large eddy simulations (LES) were performed to predict the temporal temperature fluctuations in a triple jet. This is an extension of the RANS work of Choi and Kim [15]. While RANS models are not able to predict the temperature fluctuations correctly, a large eddy simulation (LES) technique has been successfully used in limited areas of nuclear applications to investigate unsteady flow and thermal fluctuations. A few examples of the use of large eddy simulations for calculating turbulent flows and heat transfer in the nuclear field are given in Grötzbach and Wörner [19] and Simoneau et al. [20]. The main objectives of this study were to assess the capability and accuracy of LES in the thermal striping study. This is, to the authors' knowledge, the first LES study of the thermal striping in a triple jet. A detailed analysis of the flow and thermal fields was carried out and the results were compared with the available experimental data.

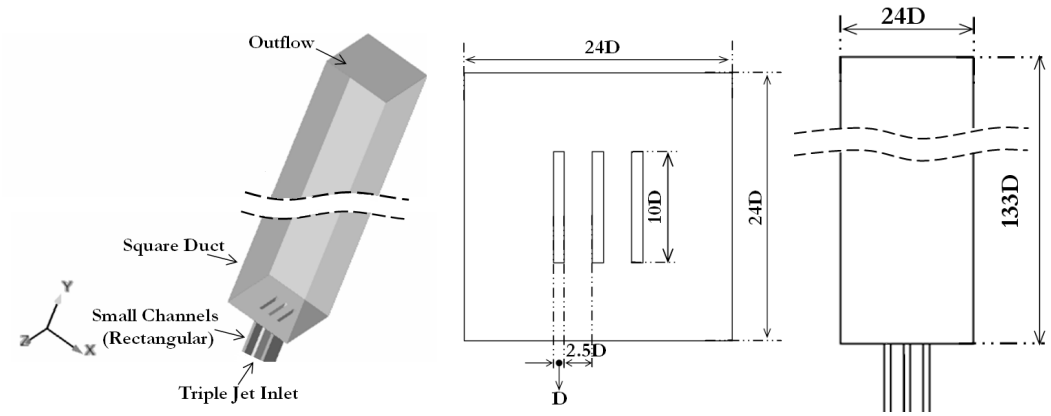

Figure 1: a) A schematic diagram of triple jet geometry, b) top view, and c) side view.

2 Triple jet

In this study, a simplified triple jet geometry was considered for numerical simulations to model the thermal striping phenomenon in the upper plenum of liquid metal fast reactor. The triple jet geometry was chosen to be the same as in the experiments of Nam and Kim [10], and was also very similar to the model used in Kimura et al. [7–9]. The geometry of the triple jet and the computational domain are given in Figure 1. The computational domain was composed of three inlet channels and a main square duct. The three channels were attached to the the base of the square duct, and the jets were issued from the nozzle. The experiment of Nam and Kim [10] was designed to be two-dimensional by using nozzles with a rectangular cross section, and the previous numerical studies used a two-dimensional grid [13–15]. In this study, we performed full three-dimensional numerical simulations using the LES technique.

All the geometric quantities were normalised with the nozzle width, D, equal to 0.015 m. The rectangular cross section of the nozzle was $D \times 10D$, and the corresponding hydraulic diameter was $D_h = 1.82D$. The gap between the neighbouring rectangular

nozzles was $2.5D$, and this was the same as the value used in Kimura et al. [7–9]. The cross section of the square duct ($24D \times 24D$) was identical to the test section used in the experiments [10]. The main square duct was $133D$ long, and this was long enough to capture the downstream behaviour of triple jet mixing. As for the coordinates, y is the jet downstream direction, z is the spanwise direction along the nozzle length, and x is orthogonal to y and z directions, so that $z/D = 0$ is the mid-span. The origin of the coordinate is located at the centre of the hot jet nozzle, and the cold jet centres are located at $x/D = \pm 3.5$.

The numerical simulations were concerned with the thermal mixing of an heated central jet (referred to as hot jet) in between two adjacent unheated jets (referred to as cold jet) at a lower temperature. The inlet temperature of the hot jet was $T_h = 65$ °C, while the two cold jets had a lower inlet temperature of $T_c = 41$ °C; the discharge temperature difference between the hot and cold jets was $\Delta T = 24$ °C. The exit velocities at the three nozzles of the triple jet were all equal to $U_j = 10\, m/s$. As air viscosity changes with temperature, the Reynolds numbers based on the nozzle width and the nozzle exit velocity were $Re_D = U_j D/\nu = 7900$ and 8800 for hot and cold jets, respectively. The Grashof number in the simulation was $Gr = 1.1 \times 10^4$, so the triple jet flow is dominated by forced convection, as is in a typical LMFR.

3 Numerical simulation

3.1 Large eddy simulation and RANS models

In LES, the Smagorinsky-Lilly model was used to model the sub-grid scale (SGS) stress tensor ($\tau_{ij} = \overline{u_i u_j} - \overline{u}_i \overline{u}_j$). The SGS stress tensor is modelled as a linear function of the large-scale strain rate tensor, S_{ij}:

$$\tau_{ij} - \frac{1}{3}\delta_{ij}\tau_{kk} = -2\nu_{SGS}S_{ij}, \tag{1}$$

$$S_{ij} = \frac{1}{2}\left(\frac{\partial \overline{u}_i}{\partial x_j} + \frac{\partial \overline{u}_j}{\partial x_i}\right), \tag{2}$$

where $\nu_{SGS} = L_s^2 \left|\overline{S}\right|$ is the SGS viscosity, and $\left|\overline{S}\right| \equiv \sqrt{2\overline{S}_{ij}\overline{S}_{ij}}$. L_s is the length scale for SGS and defined as $L_s = \min(\kappa d, C_s\Delta)$, where the Kármán constant is $\kappa = 0.42$, and d is the distance to the closest wall. The value of the Smagorinsky constant is chosen as $C_s = 0.1$, which has been proven to yield good results for a wide range of flow conditions [21]. The grid filter width is defined as $\Delta = V^{1/3}$, where V is the volume of the computational cell.

In addition to LES, two turbulence models were also considered in the present study. Spalart-Allmaras (SA) model [22] was chosen as a relatively simple one-equation model. The SA model solves the transport equation for the turbulent viscosity, $\overline{\nu}$:

$$\frac{\partial}{\partial t}(\rho\bar{\nu}) + \frac{\partial}{\partial x_i}(\rho\bar{\nu}u_i) = G_\nu + \frac{1}{\sigma_{\bar{\nu}}}\left[\frac{\partial}{\partial x_j}\left\{(\mu + \rho\bar{\nu})\frac{\partial\bar{\nu}}{\partial x_j}\right\} + C_{b2}\left(\frac{\partial\bar{\nu}}{\partial x_j}\right)^2\right] - Y_\nu + S_{\bar{\nu}}, \tag{3}$$

where G_ν is the production of turbulent viscosity and Y_ν is the destruction of turbulent

viscosity that occurs in the near wall region due to wall blocking and viscous damping. $\sigma_{\tilde{\nu}}$ and C_{b2} are constants, and $S_{\tilde{\nu}}$ is a source term.

As a second turbulence model, the realizable k-ε (RKE) model [23] was chosen in this study. The transport equations for k and ε are:

$$\frac{\partial}{\partial t}(\rho k) + \frac{\partial}{\partial x_j}(\rho k u_j) = \frac{\partial}{\partial x_j}\left[\left(\mu + \frac{\mu_t}{\sigma_k}\right)\frac{\partial k}{\partial x_j}\right] + G_k + G_b - \rho\varepsilon - Y_M + S_k, \tag{4}$$

$$\frac{\partial}{\partial t}(\rho \varepsilon) + \frac{\partial}{\partial x_j}(\rho \varepsilon u_j) = \frac{\partial}{\partial x_j}\left[\left(\mu + \frac{\mu_t}{\sigma_\varepsilon}\right)\frac{\partial \varepsilon}{\partial x_j}\right] + \rho C_1 S\varepsilon - \rho C_2 \frac{\varepsilon^2}{k + \sqrt{\nu\varepsilon}} + C_{1\varepsilon}\frac{\varepsilon}{k}C_{3\varepsilon}G_b + S_\varepsilon, \tag{5}$$

where G_k and G_b are the generation of turbulence kinetic energy due to the mean velocity gradients and due to buoyancy, respectively. $S = \sqrt{2S_{ij}S_{ij}}$, and S_k and S_ε are source terms. σ_k and σ_ε are turbulent Prandtl numbers for k and ε, respectively. A full description of those models can be found in Spalart and Allmaras [22] and Shih et al. [23].

3.2 Numerical method

The above equations were solved using a second-order finite volume method and the PISO algorithm [24] for pressure-velocity coupling. Non-iterative time advancement (NITA) was chosen for time control with a second order implicit scheme. For discretisation, a second-order accurate bounded central differencing scheme was used. The second-order upwind scheme was used for turbulence model equations. Simulations were carried out using the finite-volume CFD code, FLUENT [21]. The three-dimensional computer model of a triple jet was constructed using ICEM [25] software, and hexahedral computational

grids were generated for the geometry shown in Figure 1.

3.3 Boundary conditions

Simulation conditions were chosen to model the triple jet experiment of Nam and Kim [10] as close as possible. Inlet boundary conditions were applied at the inlet of the three channels. The inlet temperatures of the hot and cold jets were at 65°C and 41°C, respectively. Outflow boundary conditions were applied at the computational domain exit. Adiabatic, no slip boundary conditions were applied along the side walls of the duct. It is worth noting that the previous RANS studies [14, 15] modelled only the core part of the test section using pressure boundary conditions, and excluded the side walls from the computational domain. In triple jet experiments [7–9], the duct was surrounded by fluid at room temperature. In this study, the ambient air surrounding the duct was not modelled. Instead, simple adiabatic conditions were used ignoring the heat transfer between the triple jet and the side walls. Therefore, the thermal characteristics near the side walls would be different between the simulations and the experiment. However, the main interest in this study was to assess the capability of LES to predict the temperature fluctuations observed in thermal striping, and the use of different thermal boundary conditions would not affect the thermal striping phenomenon between the hot and cold jets observed in the middle of the duct (see Figure 1). Because of this difference, the thermal field was compared with the experiment in the core region away from the side walls.

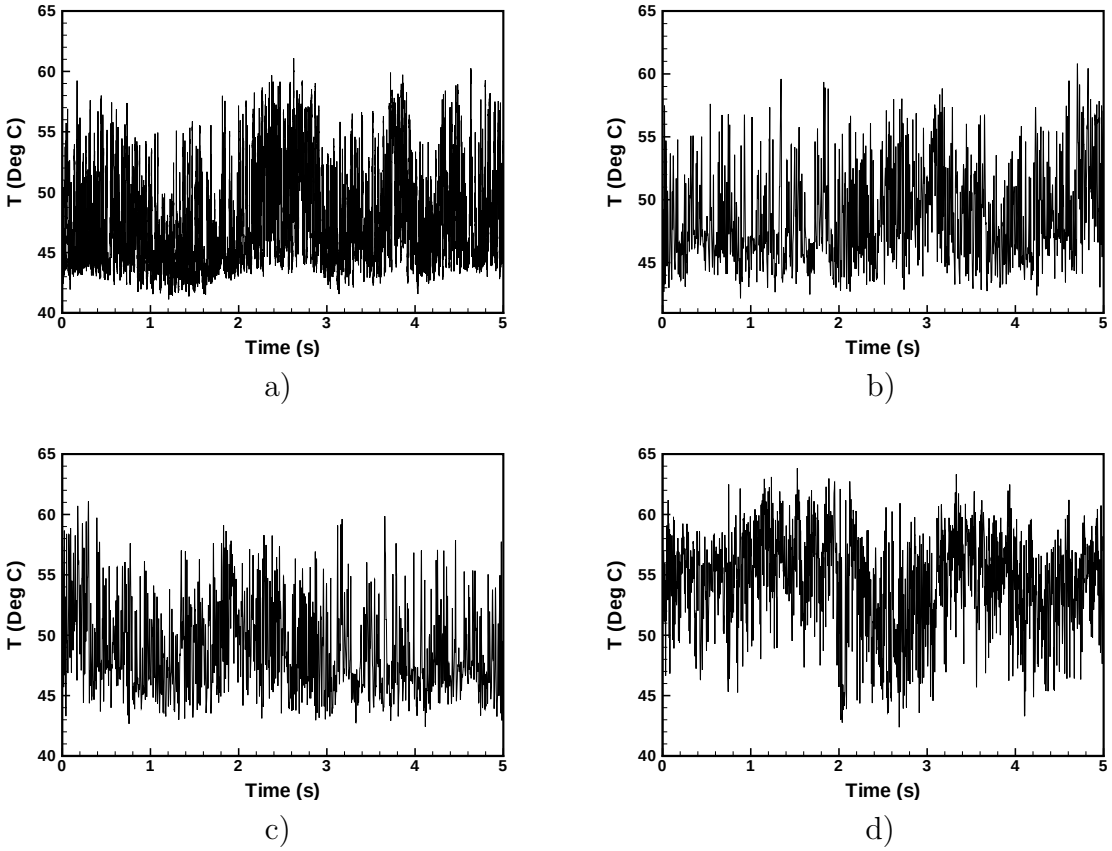

Figure 2: Time history of instantaneous temperature at the measuring point $x/D = 2$, $y/D = 15$ and $z/D = 0$: a) experiment, b) fine grid LES, c) medium grid LES, and d) coarse grid LES.

4 Results and Discussion

Several simulations were performed on different computational grids and the results were compared with the experiment of Nam and Kim [10] to ascertain the accuracy of the present LES study. Three hexahedral grids were used with 1×10^6 (coarse), 2×10^6 (medium) and 4×10^6 (fine) grid points. The first grid point was located at $0.0067D$ in the fine grid, and the near-wall model was applied in the simulations.

First, instantaneous temperature from LES with three different resolutions is monitored and compared with the experiment. Figure 2 shows the time history of temperature

Table 1: Statistical comparison of temperature data at the measuring point ($x/D = 2$, $y/D = 15$ and $z/D = 0$).

	Mean	RMS	Skewness	Kurtosis
Experiment [10]	46.5	3.3	0.97	3.2
Fine grid LES	48.3	3.4	0.74	2.9
Medium grid LES	49.1	4.6	0.72	2.6
Coarse grid LES	53.6	4.1	-0.41	2.5

at a monitoring point ($x/D = 2,\ y/D = 15$ and $z/D = 0$). The monitoring point was located between the hot and cold jets in the mid plane. Note that the centres of the hot and cold jets were located at $x/D = 0$, and $x/D = 3.5$, respectively (see Figure 1). The temperature was recorded at $1kHz$ in the LES, while the experimental data was measured at $4kHz$. The experimental data shown in Figure 2a clearly demonstrates a highly oscillating nature of the temperature fluctuations. Please note that the oscillation in the experiment is not a sinusoidal oscillation but an irregular oscillation. The peak-to-peak temperature difference is about 20°C. This is very large temperature fluctuations, given that the discharge temperature difference between the hot and cold jets is $\Delta T = 24$°C.

The temperature oscillations with three different grid resolutions are also shown in Figure 2. All three LES results correctly predict a high level of temperature fluctuations, much larger than observed in RANS studies [14, 15] (also see Figure 4). Upon close inspection, however, some differences are found between the three LES results, and the statistics are summarised in Table 1. The mean temperature in the coarse grid LES (Figure 2d) is significantly higher than the experiment, resulting in a negative value of skewness. The positive skewness of the fluctuation is correctly predicted in the medium grid LES (Figure 2c), but the amplitude of temperature fluctuations is substantially

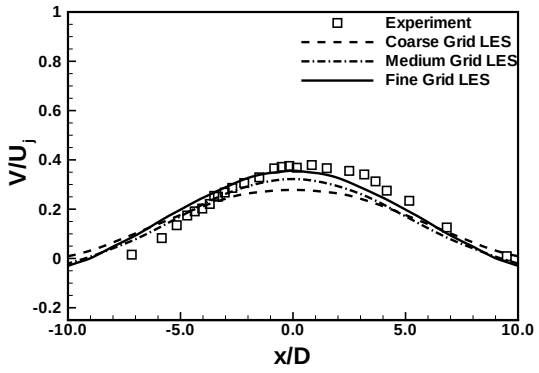

Figure 3: Grid refinement tests. The time-averaged temperature profiles in the mid-span ($z/D = 0$) at $y/D = 38$.

larger than the experiment. The results have improved further with the grid refinement, and the fine grid LES (Figure 2b) compares well with the experiment in terms of the mean, rms, skewness, and kurtosis of fluctuations although the skewness is not improved significantly. The prediction of the correct amplitude of temperature fluctuations is very important in the thermal fatigue study [1], and also is the main motivation for the use of LES in this study.

Figure 3 shows the time-averaged velocity profiles at $y/D = 38$ in the mid-span ($z/D = 0$). All three LES results predict correctly the bell-shaped velocity profile around the hot jet. The coarse grid LES under-predicts the maximum temperature due to excessive mixing between the hot and cold jets. The LES results have improved with the grid refinement, and the under-prediction has been reduced. The velocity distribution and its peak value predicted in the fine grid LES show good agreement with the experiment. It is found from the grid refinement tests that the resolution in the fine grid LES is adequate to predict the correct amplitude of temperature fluctuations of thermal striping observed in the experiment. In the following sections, the fine grid LES results are further analysed

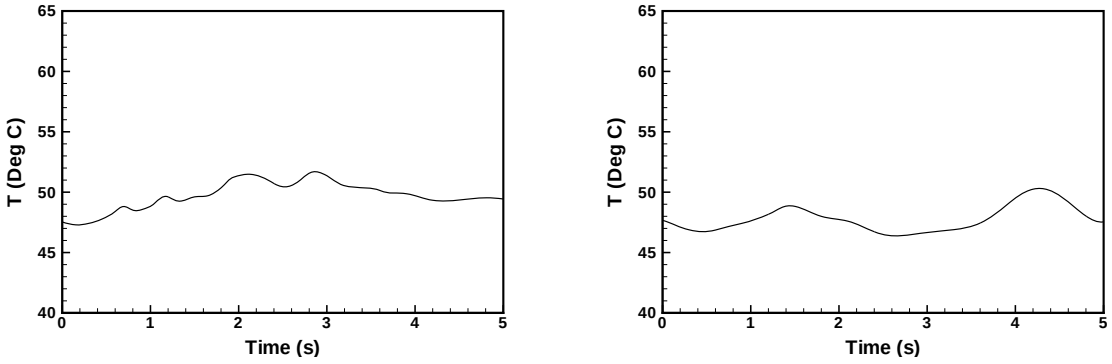

a) b)

Figure 4: Time history of instantaneous temperature at the measuring point $x/D = 2$, $y/D = 15$ and $z/D = 0$: a) SA model, and b) realizable $k - \varepsilon$ model.

to investigate the thermal and flow field of the triple jet.

4.1 Instantaneous temperature fluctuations

The time history of temperature fluctuation predicted by the SA and realizable $k - \varepsilon$ turbulence models is shown in Figure 4. The incapability of the two turbulence models to predict the oscillatory behaviour associated with thermal striping is clearly evident. The RANS results produce some level of temperature variations but fail to predict the large amplitude temperature fluctuations observed in the experiment (Figure 2a). These results are only marginally better than the two-dimensional RANS simulations of Choi and Kim [15], where the two-layer turbulence model [26] resulted in a steady state flow. It should be noted here that improved results were reported with a few turbulence models. High frequency thermal oscillations, albeit small amplitude, were predicted with the $\overline{v^2} - f$ and SST $k-\omega$ models [15]. Nishimura and Kimura [13] used a low Re number second-moment closure model to predict the low frequency periodic oscillation of a triple jet at $y/D = 5$,

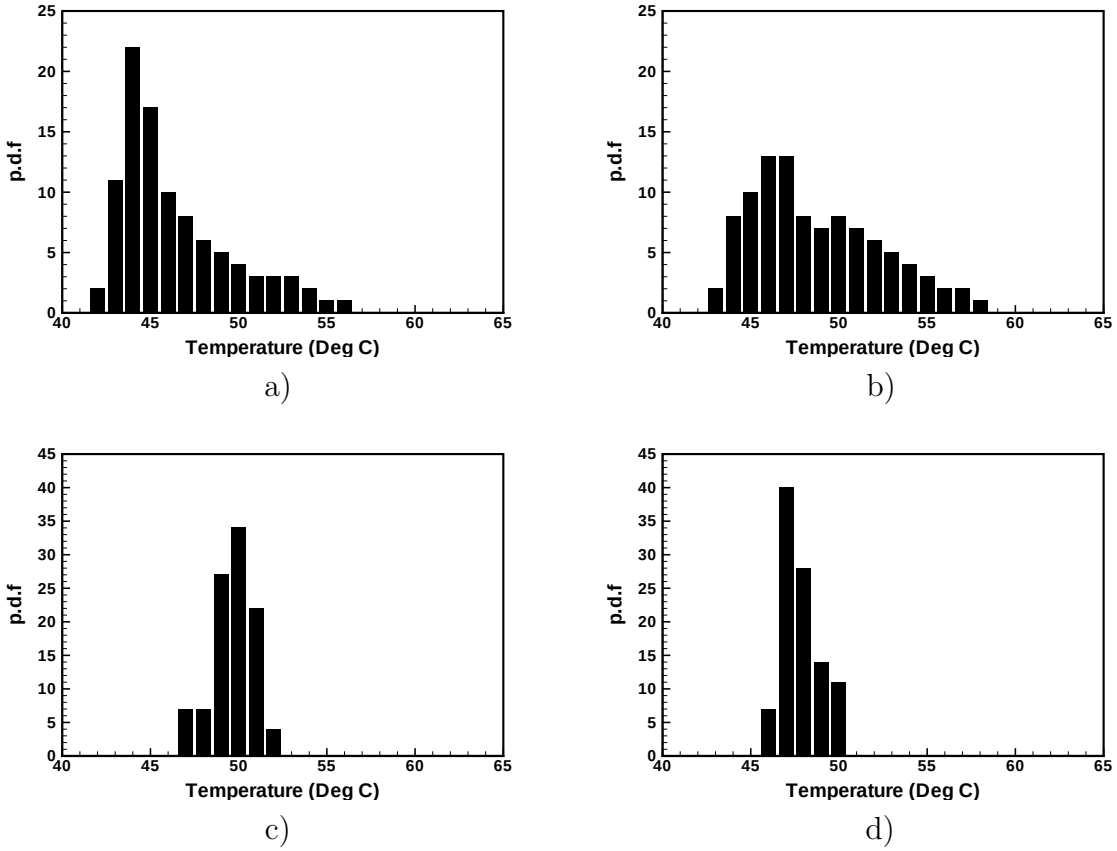

Figure 5: Probability density functions (p.d.f.) of temperature fluctuations at the measuring point $x/D = 2$, $y/D = 15$ and $z/D = 0$: a) experiment, b) LES, c) SA model, and d) realizable $k - \varepsilon$ model.

but the flow field was perfectly periodic, and the phase-averaged temperature profiles were over-predicted. The tendency of turbulence models to produce an oversimplified unsteady flow field was previously reported. For example, a laminar like vortex shedding was observed in a super-critical Re number circular cylinder flow with the standard $k - \varepsilon$ model [27]. On the other hand, as shown in Figure 2b, the average, maximum and minimum values predicted in the fine grid LES are in good agreement with the experiment, demonstrating that LES can be used to predict large amplitude temperature fluctuations in thermal striping.

The temperature fluctuations at the monitoring point are further analysed. The

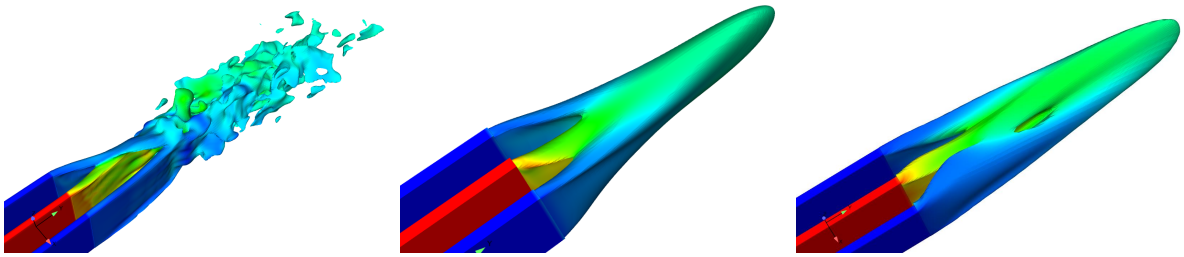

a) b) c)

Figure 6: The three-dimensional velocity contours coloured by temperature showing flow structure of the triple jet: a) LES, b) SA model, and c) realizable $k-\varepsilon$ model. Red colour indicates hot fluid and blue colour cold fluid.

probability density functions (pdf) from the fine grid LES and the two turbulence models are plotted in Figure 5 along with the experimental data. The pdf profile predicted in the LES is reasonably similar to the one in the experiment although the LES has a much broader peak than the experiment (see Table 1). The wide temperature range between the low and high ends is correctly captured in the LES, and the positively skewed distribution shown in the experiment is also accurately predicted, demonstrating that LES is capable of predicting the oscillatory behaviour of the thermal striping observed in experiment. On the other hand, the SA and realizable $k-\varepsilon$ models can predict neither the temperature range nor the peak temperature observed in experiment. Instead, the turbulence models have narrow distributions, indicating serious limitations of both RANS models to predict the frequency of temperature fluctuations.

4.2 Unsteady flow fields

Figure 6 shows iso-surfaces of velocity from the LES and the turbulence models. The surfaces are coloured by temperature. The unsteady, intermittent nature of flow field is clearly seen in the LES. The hot and cold fluid jets become unstable due to the Kelvin-

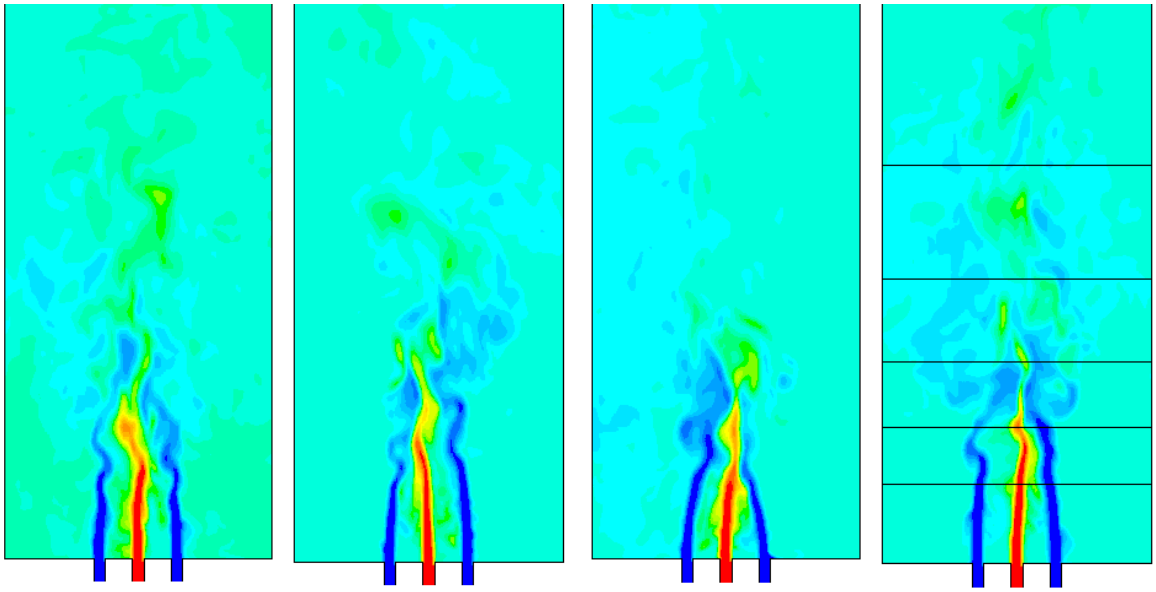

Figure 7: Instantaneous temperature contour plots of LES results in the mid-plane at several time instants. Horizontal lines inserted indicate $y/D = 7$, 12, 18, 25 and 38.

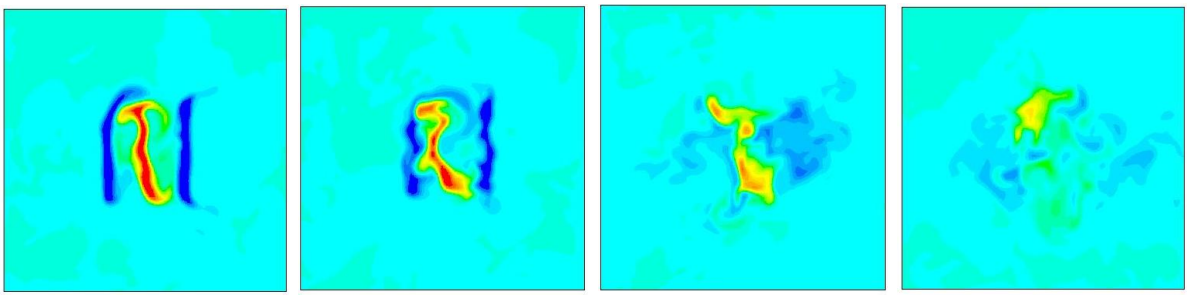

a) b) c) d)

Figure 8: Snapshots of temperature from the LES results at four cross sections, $y/D = 7$, 12, 18 and 25 from left to right, respectively.

Helmholtz instability, and interact to form vortices that travel downstream. In contrast, unsteady flow structures are missing in the flow field predicted by both turbulence models, again indicating the inability to predict the thermal striping phenomenon.

The instantaneous 2D temperature field of the LES is then analysed. Several snapshots ($24D \times 50D$) of temperature in the mid-plane are shown in Figure 7. The oscillatory behaviour of the triple jet is well captured in the LES. Similar unsteady flow patterns were observed in the thermal striping experiments [7, 12]. As the jets are issued vertically

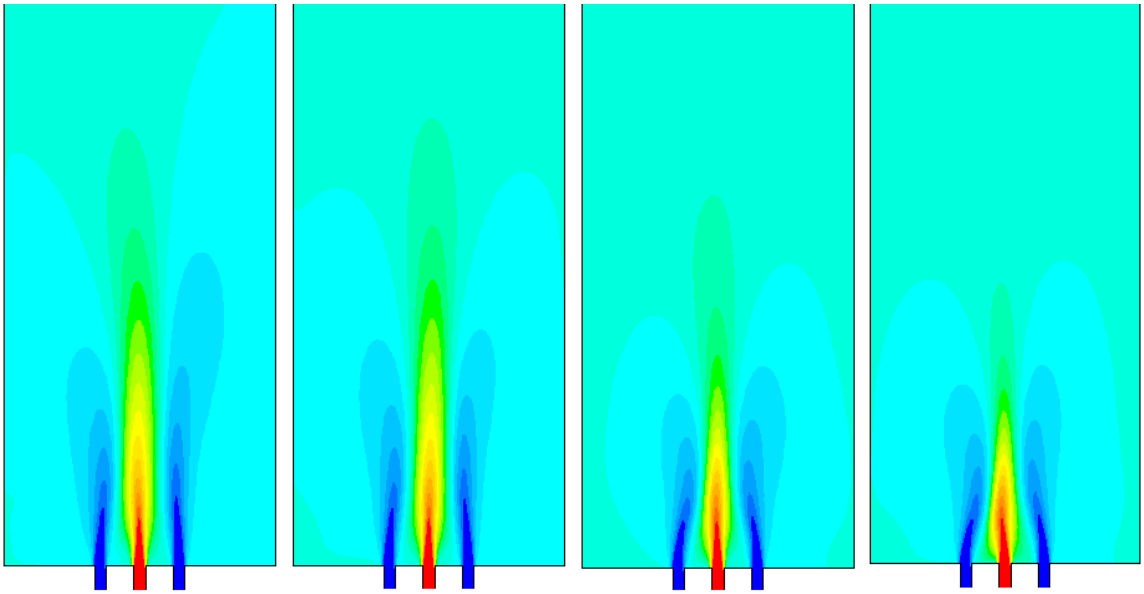

Figure 9: Instantaneous temperature contour plots of the SA model in the mid-plane at several time instants.

from the nozzles, the shear layers start to oscillate due to the shear layer instability. It is shown that the downstream development of the triple jet is asymmetric. As the hot jet in the middle oscillates laterally, the interaction with one cold jet becomes stronger than the other cold jet. This flapping motion results in an asymmetric development of downstream mixing. As the lateral motion continues, the hot jet becomes closer to alternate cold jets and starts to merge together (see also Figure 8b).

Figure 8 shows snapshots of the LES temperature at axial cross sections ($24D \times 24D$). Four downstream locations $y/D = 7$, 12, 18, and 25 are chosen to cover the wide range of downstream jet development, and these locations are indicated in Figure 7. As shown in Figure 8a, the instability starts to grow from the both ends of the rectangular jets, and the hot jet in the middle is no longer symmetric but rotates in an anticlockwise direction. The rectangular shape of the cold jets is still discernible at $x/D = 7$. It is clearly seen in Figure 8b that the flapping motion observed in Figure 7 is not two dimensional; instead,

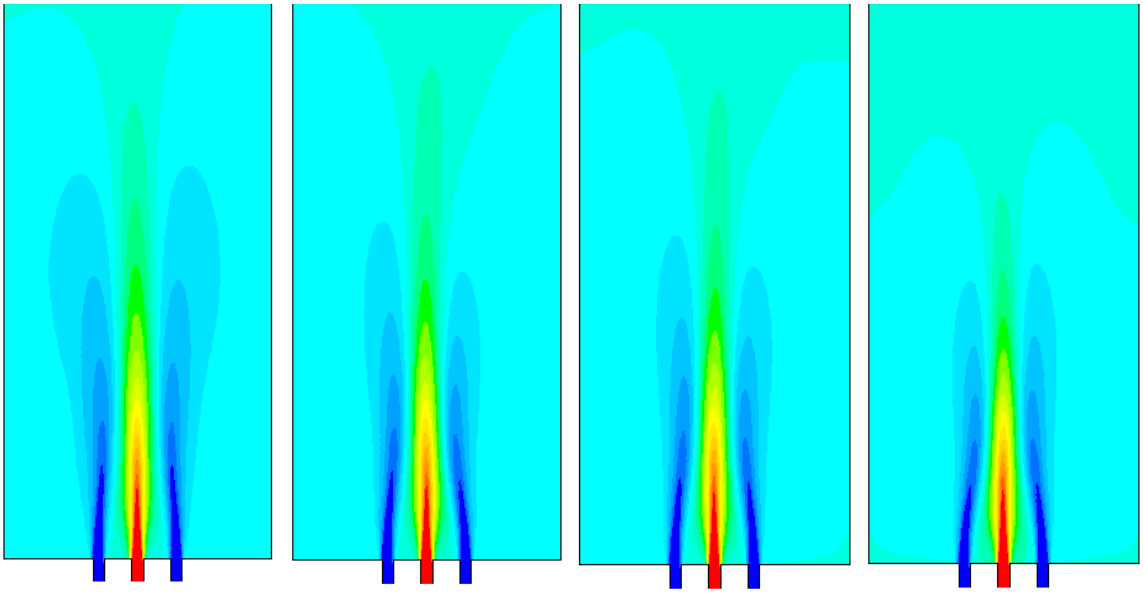

Figure 10: Instantaneous temperature contour plots of the realizable $k-\varepsilon$ model in the mid-plane at several time instants.

the jets oscillate and rotate as they move downstream. At $x/D = 12$, as the middle part of the hot jet moves to one side, the cold jet on the left hand side becomes weaker than the other cold jet due to a stronger interaction with the hot jet. As mixing continues further downstream (Figure 8c), the hot jet interacts with the cold jets on both side and the initial rectangular shape is completely lost at $x/D = 18$. The mixing is not completed at $x/D = 25$, and local areas of hot and cold fluids are still visible in Figure 8d.

Figures 9 and 10 represent snapshots of temperature in the mid-plane for the SA and realizable $k-\varepsilon$ models, respectively. The difference between the LES and the turbulence models is clearly seen. Small variations are visible in the figures but they look rather similar to the time-averaged temperature field [9, 12]. Both turbulence models are unable to predict the dynamic and oscillatory nature of the triple jet as seen in the LES and experiments [7].

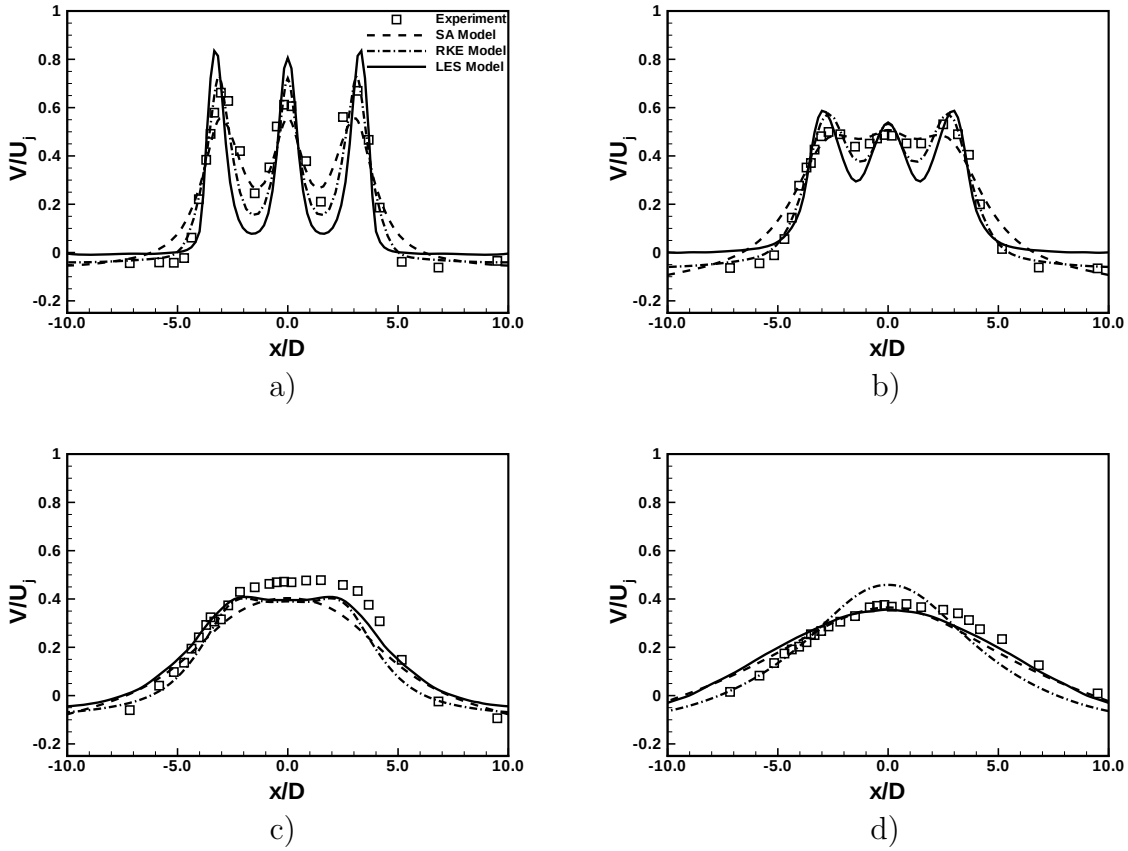

Figure 11: The time-averaged velocity profiles in the mid-span at a) $y/D = 7$, b) $y/D = 12$, c) $y/D = 18$, and d) $y/D = 38$.

4.3 Time mean quantities

The vertical mean velocity profiles across the triple jet in the mid-plane are presented in Figure 11 at four downstream locations. The LES results give good overall agreement with the experimental data. The gradual transition of the triple jet until they merges into a single jet flow is well predicted. Three peaks are still discernible at $y/D = 12$, and they merge to form a broad peak at $x/D = 18$. Further downstream at $y/D = 38$ (Figure 11d), the LES velocity profile looks very similar to a single jet profile, indicating that the mixing between the hot and cold jets is completed. The small difference between the LES and the experiment at $y/D = 38$ is partly due to the slight asymmetry of the

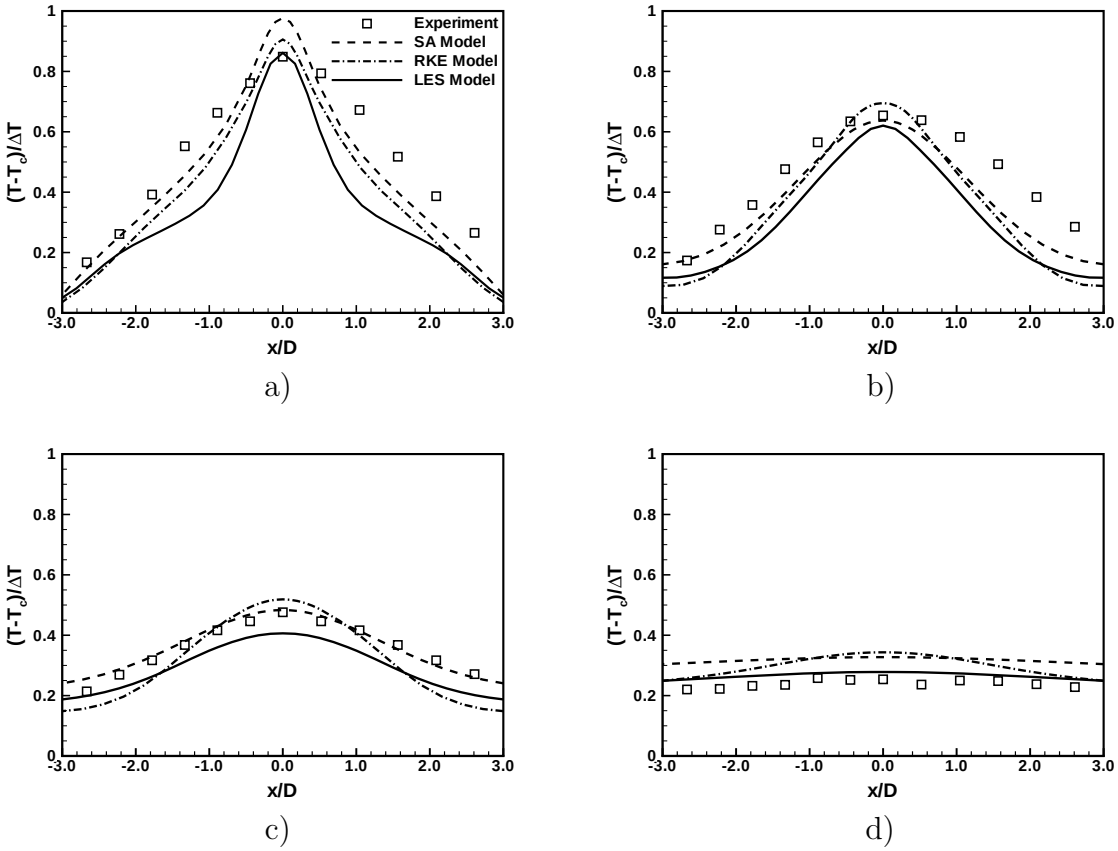

Figure 12: The time-averaged temperature profiles in the mid-span at a) $y/D = 7$, b) $y/D = 12$, c) $y/D = 18$, and d) $y/D = 38$.

experimental data. The realizable $k - \varepsilon$ (RKE) model predicts a slower downstream mixing of triple jet than the SA model, resulting in an over-prediction of the maximum velocity at $y/D = 38$. This is consistent with the thermal fields shown in Figures 9 and 10.

The mean temperatures profiles at the same downstream locations are plotted in Figure 12. Both LES and turbulence models predict the mean temperature profile generally well, and the agreement with the experiment is reasonable. It is worth noting that the LES results are worse than the RANS results at $y/D = 7$ in Figure 12a, and this is related to the slow initial development of the jets. Again, the slower mixing of the realizable $k-\varepsilon$

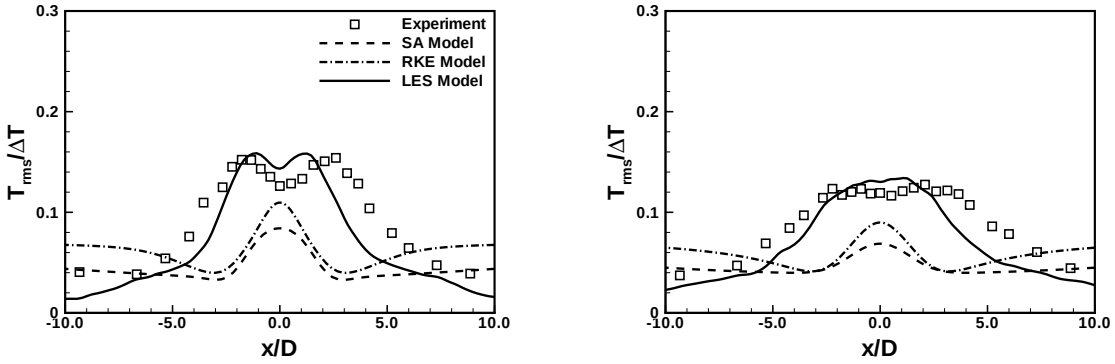

a) b)

Figure 13: The rms temperature fluctuation profiles in the mid-span at a) $y/D = 18$ and b) $y/D = 25$.

(RKE) model is evident at $y/D = 18$, where the maximum temperature is over-predicted.

The rms temperature fluctuations are presented in Figure 13. The LES results are in good agreement with the experimental data. As the jet mixing continues, the temperature fluctuations have peaks between the hot and cold jet locations as shown in Figure 13a. These double peaks are correctly predicted in the LES, while the RANS results predict only a single peak at the hot jet location. The large amplitude of temperature fluctuation is well predicted in the LES. Further downstream at $y/D = 25$ (Figure 13b), the temperature fluctuation has a broad peak, and the amplitude of temperature fluctuation is still larger than 10% of ΔT. This clearly shows that the LES can predict the correct level of temperature fluctuationx in the triple jet.

5 Conclusions

In this study, numerical simulations of a non-isothermal triple jet flow were performed to assess the capability and accuracy of LES in thermal striping study. Three different grid

resolutions were used, and the fine grid LES, which used a modest number of four million grid points, showed good agreement with the available experimental data. It is found that LES predicted the correct amplitude of temperature fluctuations, which are essential information to analyse thermal striping phenomenon. The detailed characteristics of the temperature fluctuations including skewness and kurtosis were also correctly predicted. This study has clearly demonstrated the capability and potential of LES in the thermal striping study. RANS simulations with two turbulence models were also conducted along with LES. The SA and realizable $k-\varepsilon$ turbulence models predicted the mean flow and thermal fields reasonably well although an over-prediction of the maximum values was observed with the realizable $k-\varepsilon$ turbulence model. However, the prediction of the temperature fluctuations by the two turbulence models was very poor, indicating that LES not RANS is the appropriate tool to predict the coolant temperature fluctuations associated with high-Reynolds number turbulent thermal mixing in LMFR.

Acknowledgement

This work was supported by the Engineering and Physical Sciences Research Council (EPSRC) through the UK Turbulence Consortium (Grant EP/G069581/1). The triple jet experiment was supported by the Ministry of Education, Science and Technology of Korea.

References

[1] P. Chellapandi, S. C. Chetal, and B. Raj. Thermal striping limits for components of sodium cooled fast spectrum reactors. *Nuclear Engineering and Design*, 239:2754–2765, 2009.

[2] M. Wakamatsu, H. Nei, and K. Hashiguchi. Attenuation of temperature fluctuations in thermal striping. *Journal of Nuclear Science and Technology*, 32(8):752–762, 1995.

[3] D. Tenchine and H. Y. Nam. Thermal hydraulics of co-axial sodium jets. *AIChE Symp. Ser.*, 83(257):151–156, 1987.

[4] J. P. Moro and D. Tenchine. Mixing of coaxial jets: Comparison of sodium and air experiments. In *IAEA International Working Group on Fast Reactors, Specialist Meeting on Correlation Between Material Properties and Thermo-Hydraulics Conditions in LMFBRs*, pages 1/16–6/16, 1994.

[5] D. Tenchine and J. P. Moro. Experimental and computational study of turbulent mixing jets for nuclear reactors applications. ISTP-12, 16-20 July, Istanbul, Turkey, 2000.

[6] D. Tenchine. Some thermal hydraulic challenges in sodium cooled fast reactors. *Nuclear Engineering and Design*, 240:1195–1217, 2010.

[7] A. Tokuhiro and N. Kimura. An experimental investigation on thermal striping: Mixing phenomena of a vertical non-buoyant jet with two adjacent buoyant jets as measured by ultrasound doppler velocimetry. *Nuclear Engineering and Design*, 188(1):49–73, 1999.

[8] N. Kimura, M. Nishimura, and H. Kamide. Study on convective mixing for thermal striping phenomena (Experimental analyses on mixing process in parallel triple-jet and comparisons between numerical methods). *JSME International Journal Series B*, 45(3):592–599, 2002.

[9] N. Kimura, H. Miyakoshi, and H. Kamide. Experimental investigation on transfer characteristics of temperature fluctuation from liquid sodium to wall in parallel triple-jet. *International Journal of Heat and Mass Transfer*, 50(9-10):2024–2036, 2007.

[10] H. Y. Nam and J. M. Kim. Thermal striping experimental data. Internal report, LMR/IOC-ST-002-04-Rev.0/04, KAERI, 2004.

[11] S. Ushijima, N. Tanaka, and S. Moriya. Turbulence measurements and calculation of non-isothermal coaxial jets. *Nuclear Engineering and Design*, 122(1-3):85–94, 1990.

[12] M. Nishimura, A. Tokuhiro, N. Kimura, and H. Kamide. Numerical study on mixing of oscillating quasi-planar jets with low Reynolds number turbulent stress and heat flux equation models. *Nuclear Engineering and Design*, 202(1):77–95, 2000.

[13] M. Nishimura and N. Kimura. URANS computations for an oscillatory non-isothermal triple-jet using the $k-\varepsilon$ and second moment closure turbulence models. *International Jounal for Numerical Methods in Fluids*, 43(9):1019–1044, 2003.

[14] S.-K. Choi, H. Y. Nam, M. H. Wi, S.-O. Kim, J. C. Jo, and H. K. Choi. Evaluation of turbulence models for thermal striping in a triple-jet. In *Proceedings of the ASME Pressure Vessels and Piping Conference*, volume 4, pages 867–873, 2005.

[15] S.-K. Choi and S.-O. Kim. Evaluation of turbulence models for thermal striping in a triple jet. *ASME: Journal of Pressure Vessel Technology*, 129(4):583–592, 2007.

[16] A. Manera, H.-M. Prassera, R. Lechner, and T. Frank. Toward the prediction of temperature fluctuations by means of steady RANS for the estimation of thermal fatigue. In *13th International Topical Meeting on Nuclear Reactor Thermal Hydraulics (NURETH-13)*, 27 September-2 October, Kanazawa City, Ishikawa, Japan, 2009.

[17] G. Medic and P. A. Durbin. Toward improved prediction of heat transfer on turbine blades. *ASME: Journal of Turbomachinery*, 124:187–192, 2002.

[18] F. R. Menter. Two equation eddy-viscosity turbulence models for engineering applications. *AIAA Journal*, 32:1598–1604, 1994.

[19] G. Grötzbach and M. Wörner. Direct numerical and large eddy simulations in nuclear applications. *International Journal of Heat and Fluid Flow*, 20(3):222–240, 1999.

[20] J.-P. Simoneau, J. Champigny, and O. Gelineau. Applications of large eddy simulations in nuclear field. *Nuclear Engineering and Design*, 240:429–439, 2010.

[21] Fluent. *version 6.3.26, documentation.*

[22] P. R. Spalart and S. R. Allmaras. A one-equation turbulence model for aerodynamic flows. In *30th AIAA Aerospace Sciences Meeting and Exhibit, Reno, NV, USA*, AIAA Paper 92-0439, 1992.

[23] T.-H. Shih, W. W. Liou, A. Shabbir, Z. Yang, and J. Zhu. A new $k - \varepsilon$ eddy-viscosity model for high Reynolds number turbulent flows - Model development and validation. *Computers and Fluids*, 24(3):227–238, 1995.

[24] R. I. Issa. Solution of the implicitly discretised fluid flow equations by operator-splitting. *Journal of Computational Physics*, 62:40–65, 1986.

[25] Ansys. *ICEM CFD Hexa 12.0, documentation.*

[26] H. C. Chen and V. C. Patel. Near-wall turbulence models for complex flows including separation. *AIAA Journal*, 26:641–648, 1988.

[27] P. Catalano, M. Wang, G. Iaccarino, and P. Moin. Numerical simulation of the flow around a circular cylinder at high reynolds numbers. *International Journal of Heat and Fluid Flow*, 24:463–469, 2003.